

Growth of epitaxial CoSi_2 on $\text{SiGe}(001)$

Cite as: Journal of Applied Physics **86**, 1355 (1999); <https://doi.org/10.1063/1.370894>
Submitted: 27 October 1998 • Accepted: 15 April 1999 • Published Online: 16 July 1999

B. I. Boyanov, P. T. Goeller, D. E. Sayers, et al.



View Online



Export Citation

ARTICLES YOU MAY BE INTERESTED IN

[Low-temperature formation of \$\text{CoSi}_2\$ in the presence of Au](#)

Journal of Applied Physics **95**, 5340 (2004); <https://doi.org/10.1063/1.1691180>

[Growth of single-crystal \$\text{CoSi}_2\$ on \$\text{Si}\(111\)\$](#)

Applied Physics Letters **40**, 684 (1982); <https://doi.org/10.1063/1.93234>

[Growth of epitaxial \$\text{CoSi}_2\$ on \$\(100\)\text{Si}\$](#)

Applied Physics Letters **58**, 1308 (1991); <https://doi.org/10.1063/1.104345>

Journal of
Applied Physics

SPECIAL TOPIC:
Shock Behavior of Materials

Submit Today!



Growth of epitaxial CoSi_2 on $\text{SiGe}(001)$

B. I. Boyanov, P. T. Goeller, D. E. Sayers,^{a)} and R. J. Nemanich

Department of Physics and Department of Materials Science and Engineering, North Carolina State University, Raleigh, North Carolina 27695

(Received 27 October 1998; accepted for publication 15 April 1999)

A technique for achieving epitaxial growth of (001)-oriented CoSi_2 on strained epitaxial layers of $\text{Si}_{1-x}\text{Ge}_x(001)$ is described. The technique is based on a variation of the template method, and is designed to control the local environment of Co atoms at the $\text{CoSi}_2/\text{SiGe}$ interface. The effects of the Co–Ge interactions on the interfacial reaction and the epitaxial orientation and the morphology of the silicide film were investigated. This reaction was found to cause pitting in (001)-oriented CoSi_2 films, and to stabilize the $(2\bar{2}1)$ orientation for films codeposited under conditions where $\text{CoSi}_2(001)$ growth is achieved on $\text{Si}(001)$ substrates. The $(2\bar{2}1)$ -oriented CoSi_2 films were islanded after annealing at 700 °C. The islands were terminated by (111) and (110) facets inclined at 15.8° and 19.5°, respectively, from $\text{CoSi}_2 [2\bar{2}1]$ towards $\text{CoSi}_2 [114]$. These results were interpreted in terms of reduction of interfacial and surface energies, and geometric effects. Silicide films up to 730-Å-thick were deposited and annealed up to 900 °C. The films were stable against agglomeration, and retained tensile stress in the CoSi_2 layer after annealing at 700 °C. The rms roughness of the CoSi_2 films was comparable to that of the $\text{Si}(001)$ substrate—less than 15 Å over areas as large as $20 \times 20 \mu\text{m}^2$. Films annealed at 900 °C were severely agglomerated. © 1999 American Institute of Physics. [S0021-8979(99)06714-6]

I. INTRODUCTION

Due to its low resistivity and good thermal stability, cobalt disilicide (CoSi_2) is considered an attractive contact material for deep submicron silicon devices. Recently an effort has been made by a number of groups to evaluate the feasibility of cobalt as a contact material for silicon–germanium (SiGe) devices.^{1–8} However, the development of low-resistivity CoSi_2 contacts to SiGe has faced substantial challenges. The products of the reaction of Co with SiGe have been shown to depend on the thickness of the Co film and the Ge concentration of the SiGe substrate.⁸ Due to preferential Co–Si bonding in the reaction zone, the formation of CoSi and CoSi_2 is accompanied by essentially complete segregation of germanium from the silicide phase.^{5,8} Coevaporation of cobalt and silicon has been proposed as a possible method for preventing the undesirable germanium segregation,¹ but has been found to result in islanding and poor thermal stability of the silicide film.⁷

Since CoSi_2 and Si have similar crystal structures and are closely lattice matched, it is possible to achieve epitaxial growth of CoSi_2 on both $\text{Si}(001)$ and $\text{Si}(111)$ substrates. However, in order to achieve single-crystal growth on $\text{Si}(001)$ the nucleation of CoSi_2 at the Co/Si interface must be carefully controlled through the use of CoSi_2 template layers⁹ or Co-rich deposition conditions.¹⁰ A template typically consists of a thin ($< 10 \text{ \AA}$) single-crystal CoSi_2 film formed by annealing a few monolayers (ML) of Co deposited directly on the surface of $\text{Si}(001)$. The template layer is then thickened to the desired final thickness by codepositing Co and Si in a 1:2 ratio at elevated temperatures.

Epitaxial growth of $\text{CoSi}_2(001)$ on $\text{SiGe}(001)$ has been previously reported by several groups. Spontaneous formation of epitaxial (001)-oriented CoSi_2 has been observed both on SiGe ^{8,11} and SiGeC .¹¹ In both cases the epitaxial regions co-existed with polycrystalline CoSi_2 and CoSi . The mechanism of this effect is not understood at the present time. Growth of single-crystal $\text{CoSi}_2(001)$ has been reported by Schäffer *et al.*, who used a template method with a thin sacrificial layer of Si between the SiGe substrate and the CoSi_2 template.¹² The sacrificial layer was grown at 550 °C, and was found to be an essential ingredient for achieving epitaxial growth on $\text{SiGe}(001)$. Films grown with that method exhibited an unusual $(\sqrt{2} \times \sqrt{2})R45^\circ$ reconstruction, which was attributed to the presence of Ge on the surface of the silicide.¹²

Previous studies of the CoSi_2 – SiGe interface have demonstrated a strong preference for Co–Si bonding over Co–Ge bonding.¹³ Indirect evidence that the CoSi_2 – SiGe interface energy increases approximately linearly with Ge content has also been reported.⁸ These two effects may be the cause of the observed poor thermal stability of CoSi_2 films codeposited on $\text{SiGe}(001)$,⁷ and the need to use sacrificial Si layers with template methods.¹² The preference for Co–Si bonding will hinder the formation of a continuous CoSi_2 template with conventional template methods, where the initial Co layer reacts directly with the underlying substrate. In addition, the enhanced interfacial energy of the direct Co– SiGe contact will degrade the thermal stability of the interface, and could ultimately cause the failure of the conventional template method to produce thermally stable CoSi_2 layers on $\text{SiGe}(001)$. Similar conclusions can be reached about Co-rich deposition methods.

^{a)}Electronic mail: dale_sayers@ncsu.edu

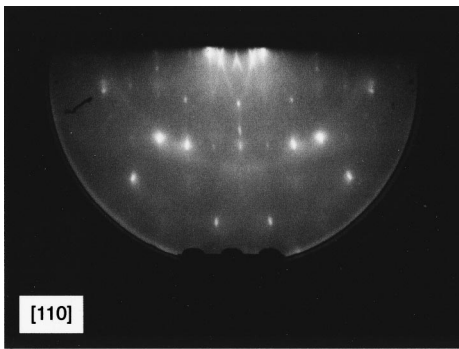


FIG. 1. RHEED pattern for a 180-Å-thick CoSi_2 film stoichiometrically codeposited directly on the $\text{Si}_{0.79}\text{Ge}_{0.21}(001)$ surface. The electron beam was incident along the $\text{Si}[110]$ azimuth. No discernible pattern was visible along the $\text{Si}[100]$ azimuth.

A natural extension of the template method is then to prevent interaction of the template with the SiGe substrate through the use of thin sacrificial Si layers between the initial Co layer and the SiGe substrate. However, deposition of Si on SiGe at 550 °C results in a Ge-denuded zone at the SiGe–Si interface, and a Ge-rich surface layer that is several monolayers thick.¹⁴ Our own measurements have shown that the characteristic (2×8) reconstruction of the SiGe(001) surface persists even after capping it with as much as 20 Å of Si at 550 °C. Therefore, methods that rely on deposition of the template and/or sacrificial layer at elevated temperatures, such as those proposed in Refs. 13 and 15, are not likely to completely prevent the undesirable interaction between Co and Ge. As will be demonstrated in Sec. III, this problem can be avoided when a modified template is deposited at room temperature. It will also be shown that codeposition using a Co-rich stoichiometry directly on the SiGe(001) surface does not promote the growth of (001)-oriented CoSi_2 , as it does on Si(001). Instead, it leads to the formation of faceted epitaxial (221) islands. A qualitative explanation of this effect based on the geometry at the $\text{CoSi}_2(221)\|\text{Si}(001)$ interface is proposed in Sec. IV.

II. EXPERIMENT

The samples used in this work consisted of 500-Å-thick strained epitaxial $\text{Si}_{0.79}\text{Ge}_{0.21}$ films grown with molecular beam epitaxy (MBE) at 550 °C on boron-doped Si(001) sub-

strates. The resistivity of the substrates was 0.8–1.2 Ω cm. The SiGe layers were not intentionally doped. Atomically clean surfaces were prepared by spin etching the Si(001) substrates with a 1:1:10 HF:H₂O:ethanol solution, followed by *in situ* thermal desorption at 900 °C, and deposition of a 200-Å-thick homoepitaxial Si buffer layer at 550 °C. The deposition was controlled with quartz crystal thickness monitors calibrated with profilometry, atomic force microscopy (AFM), transmission electron microscopy (TEM), and Rutherford backscattering (RBS). The deposition rates for all materials were below 0.5 Å/s.

Cobalt disilicide layers were grown via coevaporation of Co and Si at 400 °C with three different techniques: (a) directly on the SiGe(001) surface; (b) with a conventional CoSi_2 template; and (c) with a modified CoSi_2 template described below. In all cases several deposition stoichiometries with Si:Co ratios in the range 1.8–2.0 were examined in order to determine the effect of stoichiometry on the epitaxial alignment, morphology, and thermal stability of the silicide layer.

The conventional template approach consisted of 2 Å Co deposited on the SiGe(001) surface, capped with 2 Å Co codeposited with 7.3 Å Si.⁹ The 7.3 Å Si layer in the cap is completely consumed by the 2 Å Co layer upon annealing to form stoichiometric CoSi_2 . The modified template consisted of a 2 ML Si/1 ML Co/2 ML Si layered structure deposited sequentially on the SiGe(001) surface, capped with 2 Å Co codeposited with 7.3 Å Si. Both templates were deposited at room temperature and were then annealed to 400 °C. The silicide layers were thickened further by codepositing Co and Si at 400 °C. Unless explicitly noted otherwise, all samples discussed in this work were annealed to 700 °C for 10 min after reaching the desired final thickness. The thermal stability of selected samples was examined by annealing at temperatures up to 900 °C.

Film growth and annealing were monitored *in situ* with reflection high-energy electron diffraction (RHEED) and Auger electron spectroscopy (AES). AES data were collected with a Fisons LEG63 electron gun and a PHI 10-360 hemispherical energy analyzer. The primary beam energy and filament emission current were 5 keV and 500 μA, respectively. The annealed films were characterized *ex situ* with x-ray diffraction (XRD), AFM, TEM, and selected area diffraction (SAD). The XRD data were collected in the θ -2 θ

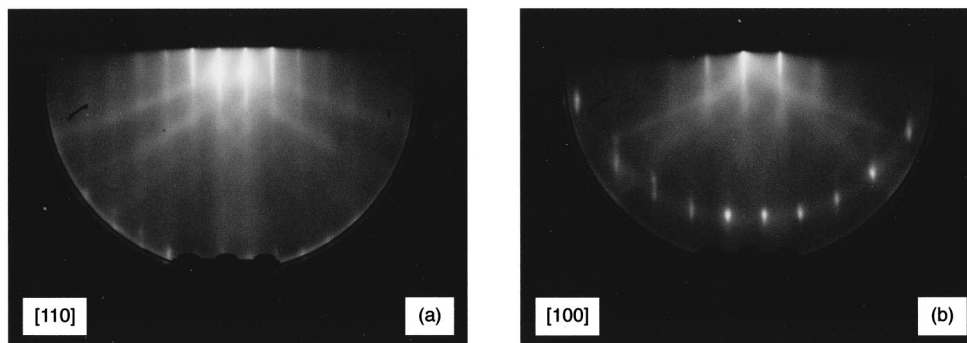


FIG. 2. RHEED pattern for a 180-Å-thick CoSi_2 film codeposited stoichiometrically on $\text{Si}_{0.79}\text{Ge}_{0.21}(001)$ with a conventional template (2 Å Co/2 Å Co + 7.3 Å Si): (a) $\text{Si}[110]$ azimuth; (b) $\text{Si}[100]$ azimuth.

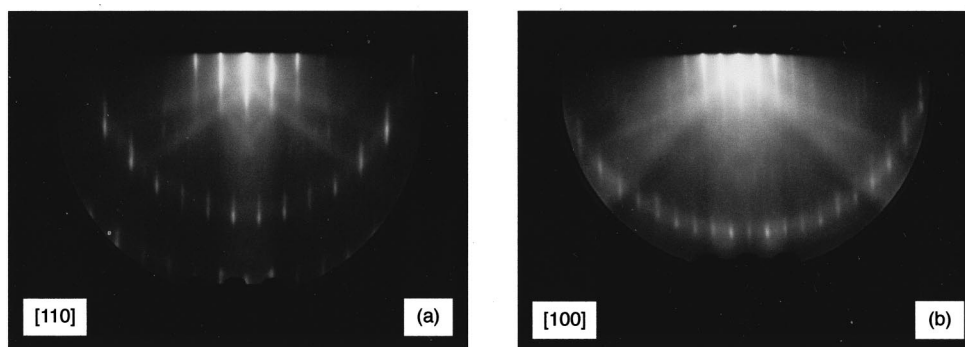


FIG. 3. RHEED pattern for a 180-Å-thick CoSi_2 film codeposited stoichiometrically on $\text{Si}_{0.79}\text{Ge}_{0.21}(001)$ with a layered template (2 ML Si/1 ML Co/2 ML Si/2 Å Co+7.3 Å Si): (a) Si[110] azimuth; (b) Si[100] azimuth.

mode between 25° and 145° 2θ with $\text{Cu } K_\alpha$ radiation on a Rigaku Geigerflex instrument equipped with a postsample graphite (0001) monochromator. The Cu anode was operated at 27.5 kV and 20 mA. AFM data were acquired in contact mode with a Park Scientific Autoprobe M5 instrument. The typical radius of curvature of the AFM tips used is reported by the manufacturer to be approximately 100 Å. The TEM images and SAD patterns were acquired with a Topcon EM-002B instrument at 200 keV. Samples were prepared for TEM by mechanical polishing from the back side followed by Ar ion milling at 12° .

III. RESULTS

A. Stoichiometric deposition

The RHEED patterns for 180-Å-thick stoichiometric CoSi_2 films prepared with the three methods described in Sec. II are shown in Figs. 1–3. The pattern for the film grown directly on the SiGe substrate consisted of weak streaks inclined at 15° – 18° with respect to the vertical (Fig. 1). The RHEED pattern for the film grown with a conventional template, shown in Fig. 2, indicated a $(\sqrt{2} \times \sqrt{2})R45^\circ$ surface reconstruction identical to that reported by Schäffer *et al.* for silicide films grown with their sacrificial template method.¹² The RHEED pattern for the film grown with the layered template is identical to the (2×2) pattern observed for $\text{CoSi}_2(001)$ growth on Si(001) (Fig. 3).^{12,16} The RHEED patterns for the templates themselves, after annealing at 400°C , are shown in Figs. 4 and 5. Nu-

merous bulk diffraction spots due to scattering from asperities on the film surface are seen in the pattern for the conventional template (Fig. 4). In contrast, the RHEED pattern for the layered template (shown in Fig. 5) displays the $(3\sqrt{2} \times \sqrt{2})R45^\circ$ reconstruction observed for the $\text{CoSi}_2/\text{Si}(001)$ S surface.¹⁶ A detailed discussion of the origin of the curved RHEED streaks is available in Ref. 16.

Ex situ AFM data collected from the three stoichiometric samples is shown in Fig. 6. The surface of the film prepared with direct codeposition consisted of elongated islands running along the $\langle 110 \rangle$ directions of the SiGe(001) substrate [Fig. 6(a)]. The two-dimensional slope histogram calculated from the image in Fig. 6(a) is shown in Fig. 7. The bright spots along the Si $\langle 110 \rangle$ directions indicate a high frequency of occurrence of these particular slopes, i.e., the surface was faceted along these directions. The facets were inclined at $15.9^\circ \pm 0.5^\circ$ and $19.8^\circ \pm 0.5^\circ$ with respect to the surface normal, and could account for the inclined streaks seen in the RHEED pattern shown in Fig. 1. Similar faceting has also been observed for films codeposited on Si(001).¹⁰

Unlike the film deposited directly on SiGe, films prepared with both template methods appeared mirror-smooth on visual inspection. The surface morphology of the two films is shown in Figs. 6(b)–6(c). The surface of the sample prepared with a conventional template consisted of smooth regions separated by deep pits that appeared to penetrate the entire silicide film [Fig. 6(b)]. A similar effect was also observed by Schäffer *et al.*¹² In contrast, the surface of the sample prepared with the layered template was virtually fea-

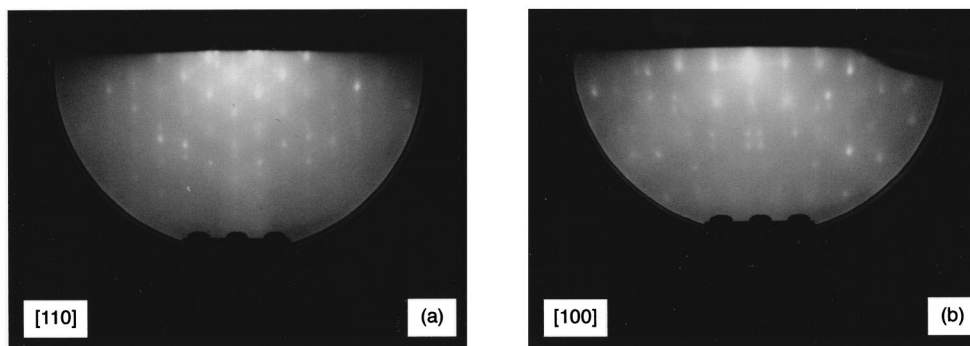


FIG. 4. RHEED pattern for a conventional template deposited on $\text{Si}_{0.79}\text{Ge}_{0.21}(001)$ and annealed at 400°C : (a) Si[110] azimuth; (b) Si[100] azimuth.

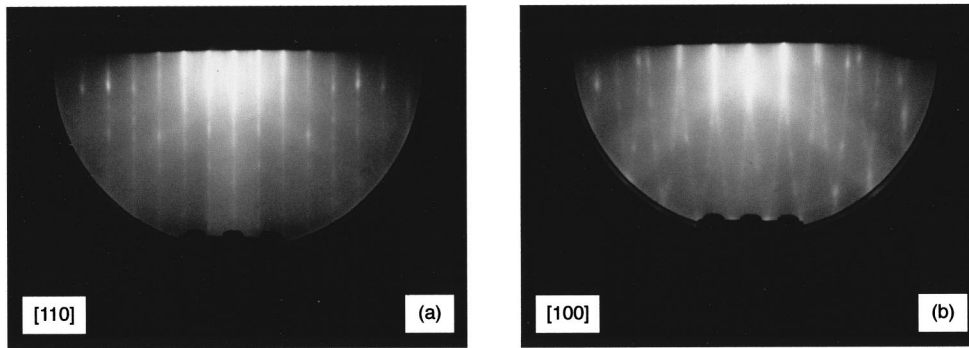


FIG. 5. RHEED pattern from a layered template deposited on $\text{Si}_{0.79}\text{Ge}_{0.21}(001)$ and annealed at 400°C : (a) Si[110] azimuth; (b) Si[100] azimuth.

tureless [Fig. 6(c)]. The rms roughness of that sample was comparable to that of the Si(001) substrate—less than 15 \AA over areas as large as $20 \times 20 \mu\text{m}^2$.

The elemental composition on the surface of the three stoichiometric samples was estimated with *in situ* AES. The estimated Ge surface concentrations for films prepared with direct codeposition, a conventional template, and a layered template were 19%, 11%, and less than 2%, respectively. It is not clear whether the small Ge signal in the sample prepared with a layered template was due to surface Ge or pinholes in the film which were not detected by AFM. Since Ge segregation on the surface of $\text{CoSi}_2(001)$ tends to stabilize the $(\sqrt{2} \times \sqrt{2})$ reconstruction,¹² the low Ge concentration observed in the sample prepared with a layered template is consistent with the (2×2) RHEED pattern shown in Fig. 3.

The crystallographic orientation of the silicide layers was examined with XRD. All peaks observed in the XRD data for the 180-\AA -thick CoSi_2 film prepared with direct codeposition were attributable to the Si(001) substrate and the SiGe(001) alloy. The crystallinity of similarly prepared and annealed films has been previously established with extended x-ray absorption fine-structure (EXAFS) measurements.⁷ The lack of measurable XRD peaks attributable to CoSi_2 therefore suggests that the 180-\AA -thick films are too thin and/or fine-grained for detection in our XRD system. In order to confirm this 730-\AA -thick CoSi_2 films were prepared and characterized under similar conditions. The surface reconstruction and morphology of these films were virtually

identical to those of the direct deposition films shown in Figs. 1–7. The XRD results are summarized in Fig. 8.

The XRD for the 730-\AA -thick CoSi_2 film prepared with direct codeposition exhibited a weak $\text{CoSi}_2(200)$ peak [Fig. 8(a)], and a broad peak at approximately 120° (not shown). The latter peak could be either the (600) or (442) peak of the CoSi_2 structure, both of which have the same d spacing and structure factor. The structure factors $|F_{hkl}|$ of the $\text{CoSi}_2(221)$, (200), (400), and (600)/(442) reflections are 0, 6.4, 121.9, and 1.4, respectively. Therefore the absence of strong $\text{CoSi}_2(200)$ and (400) peaks in Fig. 8(a) indicates that the peak at 120° was most likely $\text{CoSi}_2(442)$. This leads us to conclude that stoichiometric codeposition directly on the SiGe(001) surface produces epitaxial $\text{CoSi}_2(22\bar{1})\|\text{SiGe}(001)$ islands, in agreement with results for growth on the Si(001) surface.¹⁰

Intense $\text{CoSi}_2(200)$ and (400) peaks were clearly visible in the XRD scans of the samples prepared with templates [Figs. 8(b)–8(c)]. Since these peaks are normally weak in the CoSi_2 powder diffraction pattern (2% and 17%, respectively¹⁷), we interpret this as evidence that the CoSi_2 layer is predominantly (001) oriented. There were no quantifiable differences between the XRD results for the sample prepared with the conventional and layered templates. No other peaks besides those shown in Fig. 8 were detected in the range $25^\circ \leq 2\theta \leq 100^\circ$.

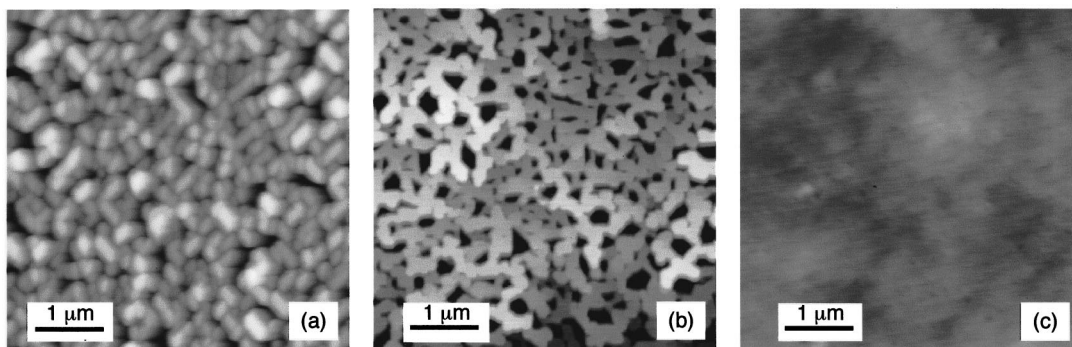


FIG. 6. AFM scans of 180-\AA -thick CoSi_2 films codeposited stoichiometrically on $\text{Si}_{0.79}\text{Ge}_{0.21}(001)$: (a) with direct codeposition; (b) with a conventional template; (c) with a layered template. The horizontal of the image is along the $\langle 100 \rangle$ direction of the Si(001) substrate. The scan size is $5 \times 5 \mu\text{m}$. The black-to-white scales are 925, 538, and 60 \AA , respectively.

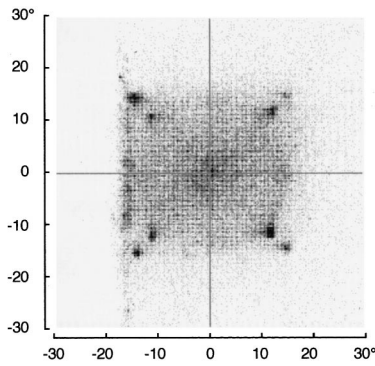


FIG. 7. Two-dimensional slope histogram calculated from the image in Fig. 6(a). The horizontal of the image is along the $\langle 100 \rangle$ direction of the Si(001) substrate. The dark spots along $\langle 110 \rangle$ are inclined at $15.9^\circ \pm 0.5^\circ$ and $19.8^\circ \pm 0.5^\circ$ with respect to the surface normal, which is at the center of the image.

The out-of-plane lattice constants of the 730-Å-thick silicide layers prepared with the conventional and layered templates were determined from the XRD results to be 5.322 ± 0.001 and 5.319 ± 0.001 Å, respectively. The lattice constant of bulk CoSi_2 is 5.367 Å, suggesting that 730-Å-thick silicide layers grown with both methods were under tensile stress in the plane of the interface. The out-of-plane lattice constants of similarly prepared 180-Å-thick films were nearly identical— 5.326 ± 0.003 and 5.321 ± 0.003 Å for films grown with the conventional and layered templates, respectively. The larger error bar of these results is due to the lower signal-to-noise ratio of the data collected from the thinner films.

The in-plane lattice constant can be estimated from classical elasticity theory¹⁸ and the measured elastic constants c_{ij} of CoSi_2 .¹⁹ The estimated in-plane lattice constant was $a_{\parallel} = 5.40 \pm 0.09$ Å, where most of the uncertainty is due to the relatively low precision of the values for c_{ij} . Since the $\text{Si}_{0.79}\text{Ge}_{0.21}$ substrate is only 500 Å thick it should be fully strained, with an in-plane lattice constant equal to that of

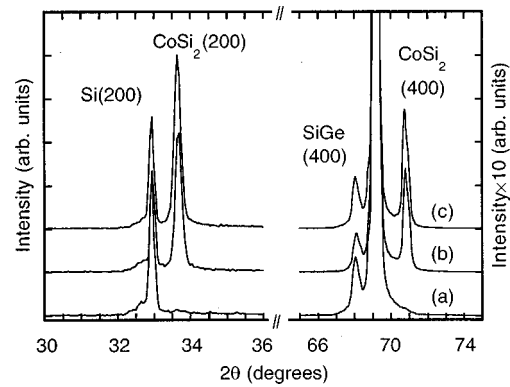


FIG. 8. XRD scans for 730-Å-thick CoSi_2 films codeposited stoichiometrically on $\text{Si}_{0.79}\text{Ge}_{0.21}(001)$: (a) with direct codeposition; (b) with a conventional template; (c) with a layered template. The unlabeled peak at $2\theta = 69.13^\circ$ is Si(400).

bulk Si, 5.4310 Å. Therefore it appears that the 730-Å-thick silicide films grown with both template methods are fully strained even after annealing at 700 °C. A similar conclusion can be reached for the 180-Å-thick films.

The grain morphology and orientation of the silicide films were also examined with plan-view and cross-section TEM and SAD. Results for the 180-Å-thick film codeposited directly on the $\text{Si}_{0.79}\text{Ge}_{0.21}(001)$ substrate are shown in Fig. 9. This SAD pattern is similar to the $\text{CoSi}_2(22\bar{1})$ pattern observed by Jimenez *et al.* for films grown on Si(001) under similar conditions, thus confirming that the silicide film directly codeposited on SiGe(001) is $(22\bar{1})$ -oriented. Spots due to all four variants of $\text{CoSi}_2(22\bar{1})\|\text{Si}(001)$ were visible. Weak spots from $\text{CoSi}_2(001)\|\text{Si}(001)$ were also detectable, indicating that the film was predominantly $(22\bar{1})$ oriented, but also contained some (001) grains. This is in agreement with the XRD results shown in Fig. 8(a). A cross-sectional micrograph of the film is shown in Fig. 10. The inclination angle of the facets relative to the interface, as measured from the micrograph, was either 15° – 16° or 18° – 19° , in agree-

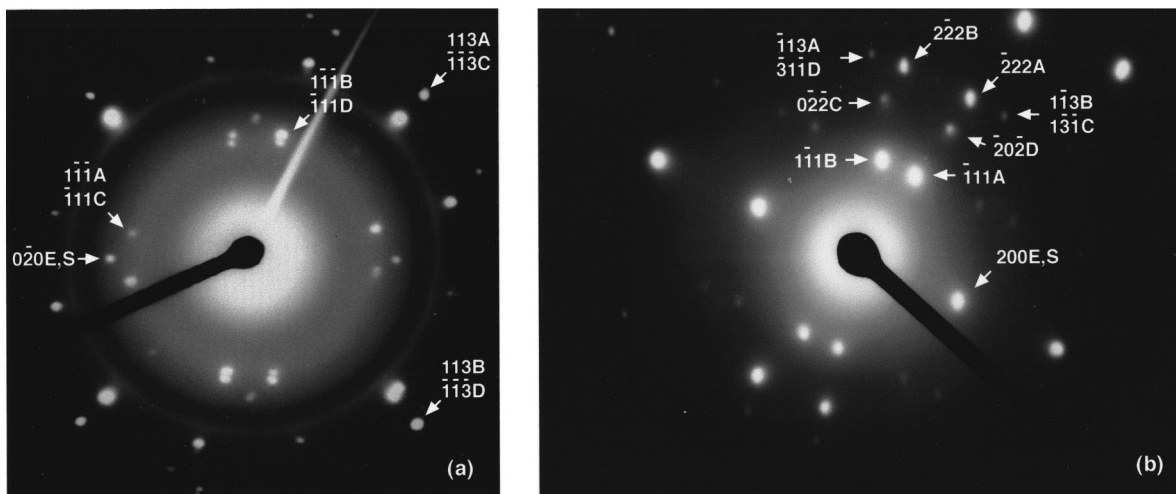


FIG. 9. TEM diffraction patterns for a 180-Å-thick CoSi_2 film stoichiometrically codeposited directly on $\text{Si}_{0.79}\text{Ge}_{0.21}(001)$: (a) with a $\text{Si}[001]$ zone axis; (b) with a zone axis tilted $\approx 12^\circ$ away from $\text{Si}[001]$ towards $\text{Si}[010]$. The labels A,B,C,D,E, and S refer to the four in-plane $\text{CoSi}_2(22\bar{1})\|\text{Si}(001)$ variants, $\text{CoSi}_2(001)\|\text{Si}(001)$, and the substrate, respectively.

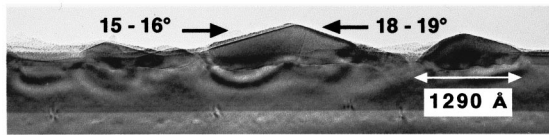


FIG. 10. Cross-sectional TEM micrograph ($\text{Si}\langle 110 \rangle$ view) of the $\text{CoSi}_2/\text{SiGe}$ interface for a 180-Å-thick CoSi_2 film stoichiometrically codeposited on $\text{Si}_{0.79}\text{Ge}_{0.21}(001)$. The longer facet of all three grains is inclined at $15^\circ\text{--}16^\circ$, and the shorter facet is inclined at $18^\circ\text{--}19^\circ$.

ment with the AFM and RHEED results discussed earlier. Note that in all cases the islands were asymmetrical, with the longer facet inclined at $15^\circ\text{--}16^\circ$, and the shorter one inclined at $18^\circ\text{--}19^\circ$.

Electron diffraction patterns and dark-field images obtained from the (200) spot for films prepared with conventional and layered templates indicated that both films were (001) oriented, with no evidence for (110) or (221) grains. The film morphologies seen in the dark-field images were consistent with those in Figs. 6(b)–6(c), confirming the earlier conclusion that the highest quality films are those grown with the layered template.

B. Cobalt-rich deposition

Several samples were prepared by codepositing Co and Si in 1:1.8 and 1:1.9 ratios onto $\text{Si}_{0.79}\text{Ge}_{0.21}$ layers. It has been reported that such conditions promote the growth of (001)-oriented CoSi_2 on $\text{Si}(001)$.¹⁰

Cobalt-rich films prepared with direct codeposition onto $\text{SiGe}(001)$ were indistinguishable from films prepared with stoichiometric codeposition, and consisted of faceted (221)-oriented islands. In contrast, epitaxial growth of atomically smooth $\text{CoSi}_2(001)$ was achieved under similar Co-rich deposition conditions on $\text{Si}(001)$.²⁰ This indicates that a Co-rich deposition stoichiometry does *not* promote the growth of (001)-oriented CoSi_2 on $\text{SiGe}(001)$.

Films prepared with layered templates under increasingly Co-rich deposition conditions exhibited degraded surface morphology, as seen by comparing Figs. 6(c) and 11. The area density of pits increased as the Si:Co deposition ratio was decreased from 2.0 to 1.8. The RHEED patterns for films grown under Co-rich conditions indicated a $(\sqrt{2} \times \sqrt{2})R45^\circ$ reconstruction identical to that shown in Fig. 2. These results suggest that the interaction between Co and the $\text{SiGe}(001)$ substrate, which occurs under Co-rich deposition

conditions, was most likely responsible for the observed pitting. However, the XRD patterns of these samples were virtually identical to those shown in Fig. 8, indicating that the silicide films preserved their (001) orientation.

It should be noted that the RHEED pattern of the annealed film was a sensitive indicator for the presence of pits. Pitting was observed in all films that exhibited a $(\sqrt{2} \times \sqrt{2})R45^\circ$ RHEED pattern. In contrast, the rms roughness of films with a (2×2) reconstruction was comparable to that of the Si substrate—approximately 10–20 Å over areas as large as $20 \times 20 \mu\text{m}^2$.

C. Thermal stability

The thermal stability of selected 180-Å-thick films grown with a layered template was tested by ramping the temperature at $20^\circ\text{C}/\text{min}$ and observing the RHEED pattern. The pattern remained unchanged from that in Fig. 3 until $850\text{--}900^\circ\text{C}$, at which point it converted to a $(\sqrt{2} \times \sqrt{2})R45^\circ$ pattern essentially identical to that shown in Fig. 2. Upon cooling to 800°C the films exhibited a (2×1) reconstruction which has not been previously reported, and which remained stable upon further cooling to room temperature. Visual inspection of the sample after annealing revealed a discoloration in the center of the wafer. However, the regions near the periphery of the wafer, which in our system can be cooler by as much as 50°C , still appeared to be mirror-smooth. AFM scans of these two regions are shown in Fig. 12. The silicide film near the center of the wafer is completely agglomerated, and consists of flat ≈ 600 Å high maze-like regions. The silicide islands run preferentially along the $\langle 110 \rangle$ directions of the substrate. As seen in Fig. 12(b), the maze-like structure appears to form as the result of nucleation and coalescence of rectangular pits at lower temperatures. The edges of the pits are also oriented along the $\langle 110 \rangle$ directions of the substrate.

As noted in Sec. III B, the appearance of a $(\sqrt{2} \times \sqrt{2})R45^\circ$ pattern is a sensitive indicator for the presence of pinholes in the film. We therefore interpret the appearance of the $(\sqrt{2} \times \sqrt{2})R45^\circ$ pattern above $\approx 850^\circ\text{C}$ as an indication of the initial breakup of the film. The (2×1) pattern observed after cooling the film to 800°C was most likely a superposition of the diffraction patterns from the center and periphery of the wafer and/or diffraction from the exposed $\text{SiGe}(001)$ substrate.

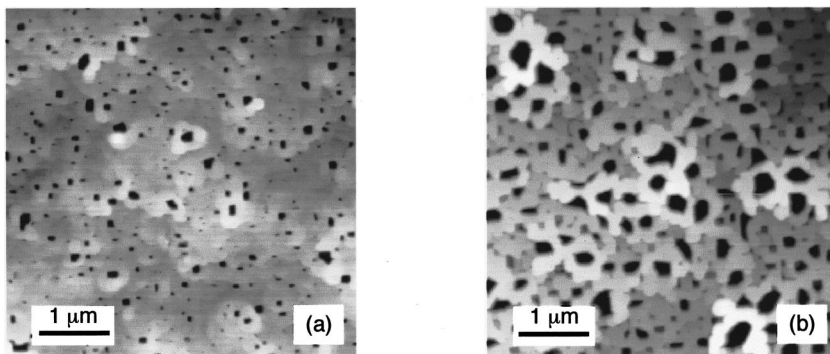


FIG. 11. AFM scans of 180-Å-thick CoSi_2 films codeposited with a layered template under Co-rich conditions on $\text{Si}_{0.79}\text{Ge}_{0.21}(001)$: (a) Co:Si $\approx 1:1.9$; (b) Co:Si $\approx 1:1.8$. The horizontal is along the $\langle 100 \rangle$ direction of the $\text{Si}(001)$ substrate. The scan size is $5 \times 5 \mu\text{m}$. The black-to-white scales are 157 and 508 Å, respectively.

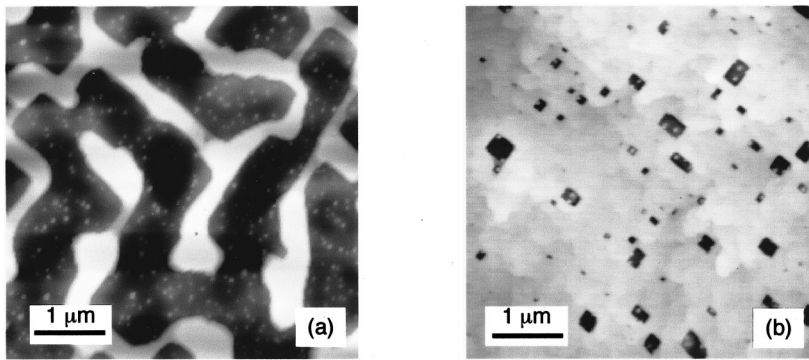


FIG. 12. AFM scans of a 180-Å-thick CoSi₂ film stoichiometrically codeposited with a layered template on Si_{0.79}Ge_{0.21}(001), and annealed to 900 °C: (a) near center of wafer; (b) at the edge of wafer. The horizontal is along the <100> direction of the Si(001) substrate. The scan size is 5×5 μm. The black-to-white scales are 1142 and 140 Å, respectively.

IV. DISCUSSION

The success of the layered template proposed here may be understood in terms of the initial stages of the reaction of Co with SiGe(001). We have recently shown that Co-Si bonds are preferentially formed when ultrathin layers of Co react with SiGe(001).¹³ Such preferential reaction precludes the formation of a continuous CoSi₂ template when Co reacts with SiGe, either because a Co layer is in direct contact with the substrate, as is the case with the conventional template method, or due to deviation of the codeposited material from a 1:2 Co:Si stoichiometry, as is the case under Co-rich deposition conditions. We have alleviated this problem by inserting a layered structure, 2 ML Si/1 ML Co/2 ML Si, at the CoSi₂/SiGe interface. This structure mimics the stacking sequence of CoSi₂ in the [001] direction and provides a sufficient amount of Si to ensure up to eightfold Co-Si coordination at the CoSi₂-SiGe interface. Deposition of the layered structure at room temperature is an important ingredient of the method, because Ge tends to diffuse through Si cap layers at elevated temperatures.¹⁴ Deposition of the template or a thin Si sacrificial layer at elevated temperatures (to maintain epitaxy), as proposed in Refs. 12 and 15, will therefore not prevent the interaction between Co and Ge, which appears to be an essential condition for the formation of smooth thermally stable epitaxial CoSi₂ films.

The faceting of the (22̄1̄)-oriented films deposited directly on the surface of SiGe(001) may be understood by examining the crystal lattice of CoSi₂ in the CoSi₂(22̄1̄) || Si(001) orientation, shown in Fig. 13. The angle of inclination of the CoSi₂ (11̄1̄) and (110) planes relative to the

Si(001) plane is 15.8° and 19.5°, respectively, in excellent agreement with the AFM results in Fig. 7. In addition, due to the lack of vertical reflection symmetry, a CoSi₂(22̄1̄) island running along the CoSi₂ [114] direction *must* be asymmetrical. If the island is terminated by (11̄1̄) and (110) facets, the longer (11̄1̄) facet will be inclined at 15.8°, while the shorter (110) facet will be inclined at 19.5°. It should be noted that all islands visible in Fig. 10 have such a structure—a long and a short facet inclined at 15°–16° and 18°–19°, respectively. This can be seen more clearly by comparing the shapes of the shaded region in Fig. 13(a) and the large island in the center of Fig. 10. We therefore conclude that codeposition on SiGe(001) results in the growth of epitaxial CoSi₂(22̄1̄) islands terminated by (11̄1̄) and (110) facets along the CoSi₂ [114] directions.

The preference for CoSi₂(22̄1̄) || Si(001) alignment in stoichiometrically deposited films may be understood qualitatively by examining the bonding at the CoSi₂(22̄1̄) || Si(001) and CoSi₂(001) || Si(001) interfaces. Since the strength of the Co-Si bond is approximately 0.52 eV lower than that of the Si-Si bond,²¹ the excess energy of the CoSi₂/Si interface will be predominantly due to replacement of Si-Si bonds with Co-Si bonds in the plane of the interface. The structure of the CoSi₂(22̄1̄) || Si(001) is not known, and there have been at least three variants proposed for the CoSi₂(001) || Si(001) interface.^{22–24} Detailed estimates of the excess energy associated with these two interfaces are therefore not possible. However, inspection of Fig. 13 reveals that the number density of Co atoms in the (22̄1̄) plane of CoSi₂ is three times lower than the corresponding number density in the (001) plane. Therefore it is reasonable to expect that the CoSi₂(22̄1̄) || Si(001) interface will have a lower density of Co-Si bonds, and therefore a lower interface energy, than the CoSi₂(001) || Si(001) interface. The fact that modest saturation of the interface with Co atoms during Co-rich deposition conditions reverts the preference to CoSi₂(001) || Si(001)¹⁰ suggests that the energy gain due to the low density of Co-Si bonds is at least partially offset by strain at the interface.

The lower density of interfacial Co-(Si,Ge) bonds at the CoSi₂(22̄1̄) || SiGe(001) interface should have a stronger stabilizing effect than it does at the CoSi₂(22̄1̄) || Si(001) interface. The Co-Si bond is approximately 0.39 eV stronger than a Co-Ge bond,²¹ and therefore a reduction in the density of Co-(Si,Ge) bonds will be favored even more, thus-

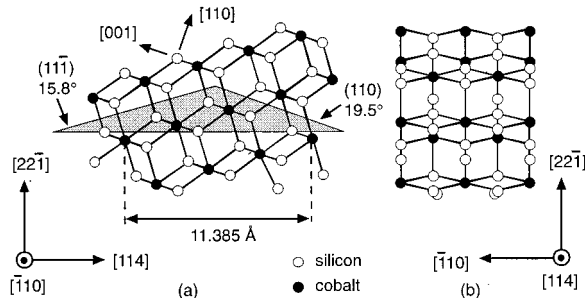


FIG. 13. Crystal structure of CoSi₂: (a) [1̄10] projection; (b) [114] projection. For the epitaxial orientation CoSi₂(22̄1̄) || Si(001) these directions are parallel to Si[110] and Si[1̄10], respectively.

perhaps explaining the persistence of the $\text{CoSi}_2(2\bar{2}1)$ orientation on the surface of $\text{SiGe}(001)$ even under Co-rich deposition conditions.

V. SUMMARY

We have studied the effect of germanium on the growth of epitaxial CoSi_2 films on $\text{SiGe}(001)$ and the stability of the CoSi_2 - SiGe interface. Growth of high-quality (001) oriented CoSi_2 films on $\text{SiGe}(001)$ could only be achieved when the bonding of the Co atoms at the interface was controlled with thin sacrificial layers. The highest quality (001) oriented films were grown with a layered template structure consisting of 2 ML Si/1 ML Co/2ML Si deposited at room temperature on the $\text{SiGe}(001)$ surface, capped with a 2 Å Co film stoichiometrically codeposited with 7.3 Å of Si. Deposition of the template at room temperature was found to be an essential condition for achieving growth of high-quality layers. Further thickening of the template was possible through codeposition of Co and Si in a stoichiometric ratio at 400 °C. The surface roughness of the films after annealing at 700 °C was comparable to that of the $\text{Si}(001)$ substrate—less than 15 Å over areas as large as $20 \times 20 \mu\text{m}^2$. Attempts to deposit (001)-oriented CoSi_2 films at Co-rich stoichiometry, either directly on the surface of $\text{SiGe}(001)$ or on a layered template, resulted in growth of $(2\bar{2}1)$ -oriented islanded films or significant pitting of the silicide layer. The $(2\bar{2}1)$ -oriented films consisted of elongated CoSi_2 islands running along the $\langle 110 \rangle$ directions of the $\text{Si}(001)$ substrate. The islands were terminated by $(\bar{1}11)$ and (110) facets inclined at 15.8° and 19.5° , respectively, from $\text{CoSi}_2 [2\bar{2}1]$ towards $\text{CoSi}_2 [114]$. The preference for $(2\bar{2}1)$ orientation during stoichiometric deposition on $\text{Si}(001)$ and $\text{SiGe}(001)$ can be understood in terms of the difference in the interface energy of the $\text{CoSi}_2(2\bar{2}1) \parallel \text{Si}(001)$ and $\text{CoSi}_2(001) \parallel \text{Si}(001)$ heterostructures. The lower density of Co–Si bonds at the $\text{CoSi}_2(2\bar{2}1) \parallel \text{Si}(001)$ interface tends to reduce its energy, making it the preferred orientation during stoichiometric deposition on $\text{Si}(001)$. Due to the lower strength of the Co–Ge bond in comparison to the Co–Si bond, the stability of this interface is enhanced even further during codeposition on the $\text{SiGe}(001)$ surface.

ACKNOWLEDGMENTS

Funding for this work was provided by DOE under Contract Nos. DE-FG05-93ER79236 and DE-FG05-89ER45384 (D.E.S.), and by NSF under Grant No. DMR-9633547 (R.J.N.).

- ¹M. C. Ridgway, R. G. Elliman, N. Hauser, and J.-M. Baribeau, *Mater. Res. Soc. Symp. Proc.* **260**, 857 (1992).
- ²H. Ying, Z. Wang, D. B. Aldrich, D. E. Sayers, and R. J. Nemanich, *Mater. Res. Soc. Symp. Proc.* **320**, 335 (1994).
- ³F. Lin, G. Sarcona, M. K. Hatalis, A. F. Cserhati, E. Austin, and D. W. Greve, *Thin Solid Films* **250**, 20 (1994).
- ⁴G. P. Watson, D. Monroe, J.-Y. Cheng, E. A. Fitzgerald, Y.-H. Xie, and R. B. Vandover, *Mater. Res. Soc. Symp. Proc.* **320**, 323 (1994).
- ⁵Z. Wang, D. B. Aldrich, Y. L. Chen, D. E. Sayers, and R. J. Nemanich, *Thin Solid Films* **270**, 555 (1995).
- ⁶M. Glück, A. Schüppen, M. Rösler, W. Heinrich, J. Hersener, U. König, O. Yam, C. Cytermann, and M. Eizenberg, *Thin Solid Films* **270**, 549 (1995).
- ⁷P. T. Goeller, B. I. Boyanov, D. E. Sayers, and R. J. Nemanich, *Mater. Res. Soc. Symp. Proc.* **440**, 487 (1997).
- ⁸B. I. Boyanov, P. T. Goeller, D. E. Sayers, and R. J. Nemanich, *J. Appl. Phys.* **84**, 4285 (1998).
- ⁹S. M. Yalisove, R. T. Tung, and J. L. Batstone, *Mater. Res. Soc. Symp. Proc.* **116**, 439 (1988).
- ¹⁰J. R. Jimenez, L. M. Hsiung, K. Rajan, L. J. Schowalter, S. Hashimoto, R. D. Thompson, and S. S. Iyer, *Appl. Phys. Lett.* **57**, 2811 (1990).
- ¹¹R. A. Donaton, K. Maex, A. Vantomme, G. Langouche, Y. Morciaux, A. St. Armour, and J. C. Strum, *Appl. Phys. Lett.* **70**, 1266 (1997).
- ¹²C. Schäffer and M. Rodewald, *J. Cryst. Growth* **165**, 61 (1996).
- ¹³B. I. Boyanov, P. T. Goeller, D. E. Sayers, and R. J. Nemanich, *Appl. Phys. Lett.* **71**, 3060 (1997).
- ¹⁴J. A. Floro and E. Chason, *Appl. Phys. Lett.* **69**, 3830 (1996).
- ¹⁵L. Haderbache, p. Wetzel, C. Pirri, J. C. Peruchetti, D. Bolmont, and G. Gewinner, *Thin Solid Films* **184**, 317 (1990).
- ¹⁶R. Stalder, C. Schwarz, H. Siringhaus, and H. von Kanel, *Surf. Sci.* **271**, 355 (1992).
- ¹⁷W. Wong-Ng, H. McMurdie, B. Paretzkin, C. Hubbard, and A. Drago, in *JCPDS-ICDD PDF-2 Database*, Ref. #38-1449 (1989).
- ¹⁸S. P. Baker and E. Arzt, in *Elastic Constants of SiGe in Properties of Strained and Relaxed Silicon Germanium*, edited by E. Kasper (INSPEC: London, 1995), pp. 67–69.
- ¹⁹G. Guénin, M. Ignat, and O. Thomas, *J. Appl. Phys.* **68**, 6515 (1990).
- ²⁰P. T. Goeller (unpublished).
- ²¹*CRC Handbook of Chemistry and Physics*, 64th ed. (Chemical Rubber Corp., Boca Raton, 1983) F176–F181.
- ²²M. F. Chisholm, N. D. Browning, S. J. Pennycook, R. Jebasinski, and S. Mantl, *Appl. Phys. Lett.* **64**, 3608 (1994).
- ²³C. W. T. Bulle-Lieuwma, A. F. de Jong, and D. E. W. Vandenhoudt, *Philos. Mag. A* **64**, 255 (1991).
- ²⁴D. Loretto, J. M. Gibson, and S. M. Yalisove, *Phys. Rev. Lett.* **63**, 298 (1989).